ACS OMEGA

http://pubs.acs.org/journal/acsodf

Article

Modification of Cellulose Ether with Organic Carbonate for Enhanced Thermal and Rheological Properties: Characterization and Analysis

Ghulam Abbas,* Abdul Haque Tunio, Khalil Rehman Memon, Aftab Ahmed Mahesar, Faisal Hussain Memon, and Ghazanfer Raza Abbasi

Cite This: *ACS Omega* 2023, 8, 25453−25466

Read Online

ACCESS | Metrics & More | Article Recommendations

ABSTRACT: Reduction in viscosity at higher temperatures is the main limitation of utilizing cellulose ethers in high thermal reservoir conditions for petroleum industry applications. In this study, cellulose ether (hydroxyethyl methyl cellulose (HEMC)) is modified using organic carbonates, i.e., propylene carbonate (PC) and diethyl carbonate (DEC), to overcome the limitation of reduced viscosity at high temperatures. The polymer composites were characterized through various analytical techniques, including Fourier-transform infrared (FTIR), H-NMR, X-ray diffraction (XRD), scanning electron microscope (SEM), thermogravimetric analysis (TGA), differential scanning calorimetry (DSC), ζ-potential measurement, molecular weight determination, and rheology measurements. The experimental results of structural and morphological characterization confirm the modification and formation of a new organic carbonate-based cellulose ether. The thermal analysis revealed that the modified composites have greater stability, as the modified samples demonstrated higher vaporization and decomposition temperatures. ζ-potential measurement indicates higher stability of DEC- and PC-modified composites. The relative viscometry measurement revealed that the modification increased the molecular weight of PC- and DEC-containing polymers, up to 93,000 and 99,000 g/moL, respectively. Moreover, the modified composites exhibited higher levels of stability, shear strength and thermal resistance as confirmed by viscosity measurement through rheology determination. The observed increase in viscosity is likely due to the enhanced inter- and intramolecular interaction and higher molecular weight of modified composites. The organic carbonate performed as a transesterification agent that improves the overall properties of cellulose ether (HEMC) at elevated temperatures as concluded from this study. The modification approach in this study will open the doors to new applications and will be beneficial for substantial development in the petroleum industry.

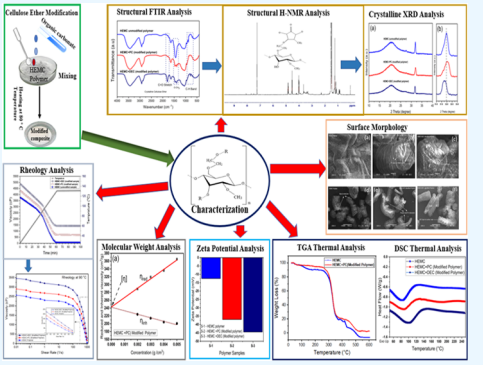

1. INTRODUCTION

Cellulose is the most abundant renewable biopolymer on Earth.[1] In recent years, cellulose and its derivatives have received increasing attention across various industrial applications due to their unique properties including biodegradability, biocompatibility, and chemical stability.[2,3] Among cellulose derivatives, cellulose ethers are particularly well-documented for their use as emulsion stabilizers, thickeners, suspension stabilizers, binders, adhesives, film formers, finishing composites, and protective colloids in different industries.[4] Furthermore, their water solubility, improved rheology, water retention, and high viscosity capabilities make them distinctive and suitable for use in the petroleum industry.[5]

Methyl cellulose (MC), hydroxyethyl cellulose (HEC), carboxy methyl cellulose (CMC), ethyl cellulose (EC), hydroxyethyl methyl cellulose (HEMC), hydroxypropyl cellulose (HPC), and hydroxypropyl methyl cellulose (HPMC) are important types of cellulose ether. Polymers and polysaccharides, both macromolecules, are widely used in the petroleum industry due to their properties such as chemical stability, nontoxicity, and solubility in water.[6,7] Cellulose ethers are used as multifunctional additives in drilling fluids and cement slurries to control fluid loss, improve rheology, and achieve other relevant properties recommended by the American Petroleum Institute (API).[5,8] However, cellulose ethers are prone to thermal thinning and viscosity loss at high temperatures. The regular structure of the molecules weakens with increasing temperature, leading to

Received: April 30, 2023
Accepted: June 19, 2023
Published: July 4, 2023

a decrease in solution viscosity due to thermal degradation.[9−11]

Polyalkylamine (PAM) and xanthan form precipitations and degrade at a high temperature greater than 80 °C.[12] HEC loses viscosity above 60 °C,[13] while partially hydrolyzed polyacrylamide (HPAM) polymer becomes unstable beyond 70 °C.[14] Starch and CMC degrade significantly above 90 °C,[15] and xanthan gum experience a drop in viscosity above 85 °C.[16,17]

Therefore, it was necessary to modify, regenerate, and synthesize the polymer to compensate for viscosity loss. There are various studies on the synthesis/regeneration of polymer to describe the development of new intermolecular hydrogen bonds to enhance the polymer properties for petroleum and other industrial applications.[18−20] In emerging green formulations, natural polymers have been synthesized to improve the API properties of drilling fluids and cement slurries, and to enhance the sweep efficiency for hydrocarbon recovery.[21] The combination of biopolymers, including CMC, hydroxypropyl starch (HPS), and xanthan, with fluid additives, showed higher and improved viscosity. However, the ζ-potential value of the synthesized polymeric solution was unstable and fluctuating, leading to its unsuitability for use in operations.[22,23] Additionally, a combination of various natural polymers has been employed in fluids as a thermal stability control and viscosity modifier agent to improve fluid properties. However, despite these benefits, polymers have certain limitations related to displacement in the wellbore.

The high viscosity of polymeric solution at normal surface conditions can increase the pump pressure and pump rate during displacement.[24,25] Furthermore, this high surface viscosity can cause operational problems such as wellbore instabilities and delays in the transportation process of drill cuttings to the wellbore surface.[26] The viscosity of the polymeric solution was increased due to the use of a higher concentration of polymer and a combination of various polymers in order to enhance the stability at higher temperatures. The higher viscosity and wellbore instability problem at surface conditions can be compensated by adding plasticizers or dispersant additives in drilling fluid and cement slurry. On the other side, a low polymer concentration may be advantageous under these conditions, but at higher temperatures, the solution's viscosity will decrease, and it would not be able to reach the fluid's desired goal. Under such circumstances, it is recommended to use ionic liquid and organic solvent to compensate for the viscosity loss of the polymeric solution at high temperatures. Ionic liquids and solvents are being used for modification and regeneration to enhance the properties of polymers.[27] However, the current regeneration methods are considered highly problematic due to toxic ionic solvents and reagents requiring multiple derivatization steps and high-temperature reactions.[28] These processes are associated with substantial environmental pollution and pose economic and environmental challenges.[29] Therefore, in recent years, there has been a search for less polluting, simpler, and more efficient energy methods to improve thermal stability and enhance the properties of solutions.[22,28,30]

Propylene carbonate (PC), ethylene carbonate (EC), diethyl carbonate (DEC), and dimethyl carbonate (DMC) are nonpolymeric cyclic and acyclic organic carbonate solvents that are minimally toxic and biodegradable.[31] These solvents have been investigated as green cosolvents for modification and are considered viable alternatives to conventional ionic liquids regarding safety and environmental impact.[32] These environmentally friendly properties of organic carbonates make them highly suitable as potential green solvents and transesterification agents for modification. In the literature, limited studies were reported on polymer composites' regeneration using organic solvents to enhance the molecular weight and viscosity of polysaccharides.[33] The literature search found that the characterization of these regenerated polymers needed to be documented. Furthermore, cellulose ether and its subsets, currently and widely used in fluids, have yet to be synthesized and modified via organic carbonate solvents to improve their properties. Previously, more research has been needed on utilizing cellulose ether and its derivative for modification, characterization, analysis, and implementation in the petroleum industry. Therefore, it is essential to comprehend the possible impact of organic carbonates on cellulose ether's modification and physicochemical properties.[34]

This research work presents the use of organic carbonate solvents to modify hydroxyethyl methyl cellulose (HEMC) cellulose ether and create new functionalized cellulose ether through a simple and fast derivatization process at mild temperatures. The novelty of this research lies in evaluating the impact of cyclic propylene carbonate and acyclic diethyl carbonate as a transesterification and green solvent agent on native HEMC cellulose ether through various characterization methods. Experimental work was conducted to modify HEMC using PC and DEC separately. The physical, thermal, structural, and morphologic characteristics were assessed using Fourier-transform infrared (FTIR), H-NMR, X-ray diffraction (XRD), scanning electron microscope (SEM), thermogravimetric analysis (TGA), and differential scanning calorimetry (DSC). Further, the impact of these organic solvents on ζ-potential (stability) and molecular weight was evaluated through the relative viscometry method. Finally, rheological studies were performed to evaluate the impact of organic carbonate as a transesterification agent on native polymer through solubility, hydration rate, and viscosity measurement by changing temperature and shear rate. The findings of this study could assist in enhancing the production process of the polymer and optimizing its performance for use in cementing and drilling fluid applications within the petroleum industry.

2. MATERIALS AND METHODS

2.1. Materials. Hydroxyethyl methyl cellulose (HEMC), a nonionic ether polymer, was obtained as a white to off-white powder with a particle size (mesh) of 80 from GANTRADE Corporation, China. The molecular weight range of the polymer was $M_w = 4 \times 10^4$ to 9×10^4 g/mol, with a degree of substitution (DOS) of 1.4 and a molecular/molar substitution (MO) of 0.2. Propylene carbonate ($C_4H_6O_3$) with a boiling point of 240 °C and a flash point of 123°C and DEC ($C_5H_{10}O_3$) with a boiling point of 126 °C and flash point of 33°C were purchased from Daejung Chemicals & Metals, Korea. The chemical structure of HEMC (cellulose ether) investigated in this study is shown in Scheme 1 in a simple manner.

2.2. Methods. The experimental setup involved modifying the polymer and conducting various characterizations. The process of modifying the polymer and evaluating its characteristics is illustrated in Figure 1.

https://doi.org/10.1021/acsomega.3c02974
ACS Omega 2023, 8, 25453−25466

Scheme 1. Chemical Structure of HEMC

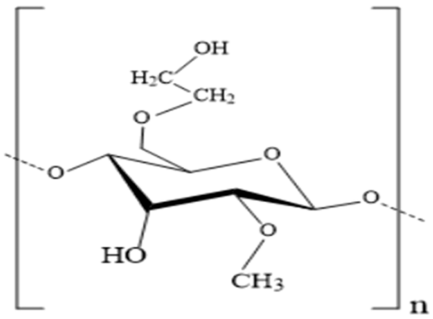

2.3. Modification of Cellulose Ether. HEMC powder was spread in a thin layer, and then, organic carbonates (PC and DEC) were dropped separately onto the grained polymer surface.[31] HEMC polymer with a molecular weight of 9×10^4 g/mol was used for modification and grafting using organic carbonate. The mixed composite was heated at 80 °C in a roller oven for 12 h to promote the chemical reaction using wet and dry methods. This synthesis process blends the HEMC polymer and organic carbonate, resulting in a final product in powder form. The weight ratio of HEMC polymer to organic carbonate was based on the optimal and minimal concentration of organic carbonate to react with cellulose. The most preferable weight ratio of polysaccharide to organic carbonate was suggested in the range of 1:0.05 to 1:0.25.[33] The optimal concentration weight ratio of HEMC with organic carbonate was confirmed through FTIR analysis. At a 1:0.20 concentration weight ratio, a significant change was observed at various wavenumbers of the transmittance spectrum. Therefore, a 1:0.2 weight ratio was used for modification.

2.4. Characterization Techniques. The functional group of cellulose ether and modified polymer samples were analyzed using a FTIR spectrophotometer (PerkinElmer). Spectra of the polymer samples were recorded in the range of 500 to 4000 cm^{-1} wavenumber with 32 scans having a 4 cm^{-1} resolution.[35] A nuclear magnetic resonance (NMR) spectrometer (600 MHz Bruker AVANCE) was used to identify the modification of cellulose ether using $CDCl_3$ as a deuterated solvent through chemical shift analysis. The spectra were expressed as chemical shifts in parts per million (ppm) with respect to signal intensity.[36] The polymeric sample structure pattern and crystallinity index (CI) were investigated using PANalytical's X-ray diffraction (XRD) instrument. The test was conducted at a scan rate of 2°/S in 2 theta (θ) diffraction angle between 10 and 40°. The deconvolution method was utilized to determine the CI of the polymeric sample using the following eq 1

$$\mathrm{CI} = \left[\frac{I_{cr} - I_{ar}}{I_{cr}}\right] \times 100\% \quad (1)$$

where I_{cr} represents the intensity of the maximum peak for the crystalline region. I_{ar} represents the minimal peak intensity of the amorphous region in XRD spectra.

A scanning electron microscope (JEOL JSM6380L) was used to analyze polymer specimens' morphology at 10 kv. Morphology image profiles of powdered polymer samples were investigated using 5 and 50 μm scale zoom size.[1]

Thermal degradation of the polymer samples was analyzed through thermal gravimetrical analysis (TGA) (PerkinElmer). For each polymer sample, 10 mg weight of polymer sample was used for thermal analysis from 30 to 600 °C with an increment rate of 10°/min under a nitrogen gas flow of 20 mL/min. The thermal behavior of polymer samples was also analyzed using differential scanning calorimetry (DSC) (PerkinElmer). The same quantity of each sample was used for DSC analysis from 30 to 200 °C with an increment rate of 10°/min under a nitrogen gas flow of 20 mL/min.

Zetasizer Nano ZS (Malvern Instruments, U.K.) was used to evaluate the ζ-potential magnitude of polymeric solutions at a temperature of 25 °C. The solutions were prepared using 0.05 wt % of the dry polymer sample in an aqueous medium with 0.1M NaOH to adjust the pH to 7.5. The pH of the sample solutions was measured using a pH meter with an accuracy of 0.01/unit at 25 ± 0.5 °C. It was observed that the pH values of HEMC solutions ranged from 7.02 to 7.50.

2.5. Polymer Solution Preparation and Molecular Weight Measurement Method. The average molecular weight (M_w) of modified composites was determined through relative viscosity measurement using a BS/U-tube viscometer. In this method, relative viscosity was determined by measuring the elapsed time (t) for the polymer solution to flow through a capillary tube and comparing it to the elapsed

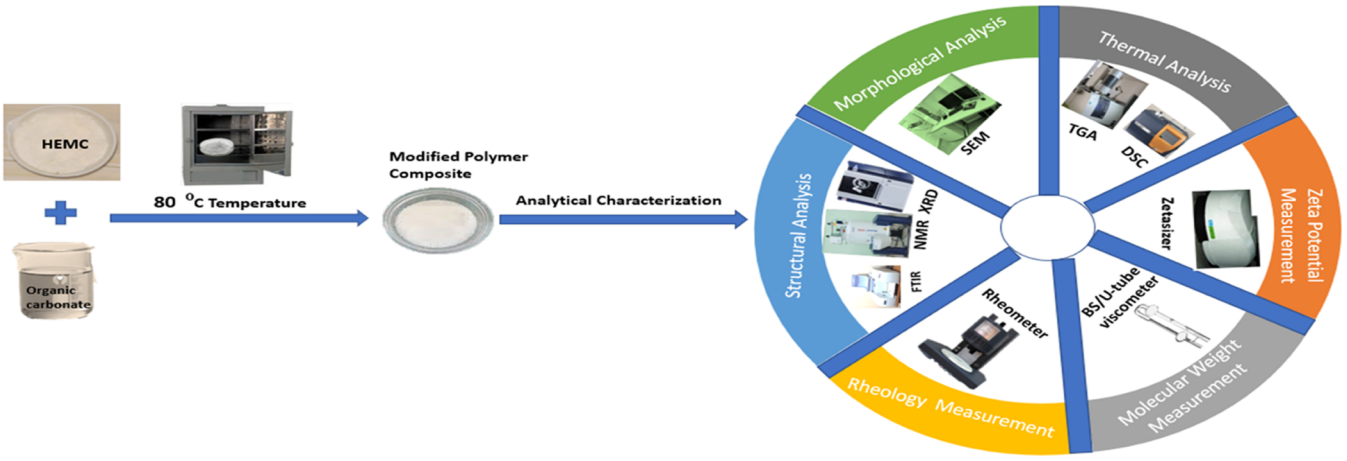

Figure 1. Schematic representation of the conceptual layout of the present work employed for modification and characterize the polymer composites. The images shown are taken at the Advanced Characterization Lab and created by the team of authors.

https://doi.org/10.1021/acsomega.3c02974
ACS Omega 2023, 8, 25453−25466

time (t_s) for the solvent to flow. Two grams of the powdered polymer was dissolved in 100 mL of deionized water and stirred for 02 h using a hot magnetic plate. The prepared polymer solution was further diluted in distilled water to prepare 0.0020, 0.0030, 0.0040, and 0.0050 gm/cm^3 solutions of modified and unmodified polymer composites. The molecular weight of the polymer solutions was determined through this relative viscometry method using the Mark–Houwink–Sakurada (MHS) equation[37,38]

$$[\eta] = K[M^a] \tag{2}$$

where $[\eta]$ represents intrinsic viscosity, "a" and "K" are the coefficient and Mark–Houwink constant for the polymer solution, and M denotes the molecular weight of the solution. The intrinsic viscosity $[\eta]$ was determined through flow curve measurements. Initially, the relative viscosity was measured as a function of polymer concentration through elapsed time using the following relationship[39]

$$\eta_r = \eta/\eta_s \approx t/t_s \tag{3}$$

where η_r is the relative viscosity, η is the viscosity, and t is the flowing time of the polymer solution. In the same way, η_s represents the viscosity and t_s is the elapsed flow time of the solvent. The relative viscosity is used to determine the specific and inherent viscosities (η_{sp} and η_{inh}) through the following equations[37]

$$\eta_{sp} = \eta_r - 1 \tag{4}$$

$$\eta_{inh} = \ln(\eta_r)/C \tag{5}$$

While using the specific viscosity, the reduced viscosity (η_{red}) was determined by the following expression

$$\eta_{red} = \eta_{sp}/C \tag{6}$$

The reduced viscosity and inherent viscosity are concentration dependent due to their nonideal behavior and phenomena.[40] Therefore, intrinsic viscosity is defined as a limit of both (η_{red}) and (η_{inh}) as $C \to 0$.

$$[\eta] = \lim_{C\to 0}(\eta_{red}) = \lim_{C\to 0}(\eta_{sp}/C) \tag{7}$$

$$[\eta] = \lim_{C\to 0}(\eta_{inh}) = \lim_{C\to 0}\ln(\eta_r/C) \tag{8}$$

In last, the intrinsic viscosity $[\eta]$ was evaluated through the plot of (η_{red}) or (η_{inh}) vs concentration and by extrapolating a straight line to $C = 0$.

2.6. Rheology Measurement. A 01 wt % concentration solution of modified and unmodified polymer samples was prepared in deionized water by stirring using a hot magnetic plate stirrer for rotational viscosity measurement. The rheology of prepared solutions was determined in terms of viscosity at various shear rates, time, and temperature range of 25–130 °C. The rheology data were evaluated using a rheometer (AR 1500, TA Instruments) with a cone and plate geometry of 40 mm diameter and a 2° angle.[36]

3. RESULTS AND DISCUSSION

3.1. FTIR Analysis. FTIR spectra of HEMC native polymer are depicted in Figure 2. The band observed at 3442 cm^{-1}, the wavenumber of 3442 cm^{-1}, is endorsed to the O–H stretching, indicating the existence of free O–H in the molecular structure.[41] From 2920 to 2517 cm^{-1}, the vibration

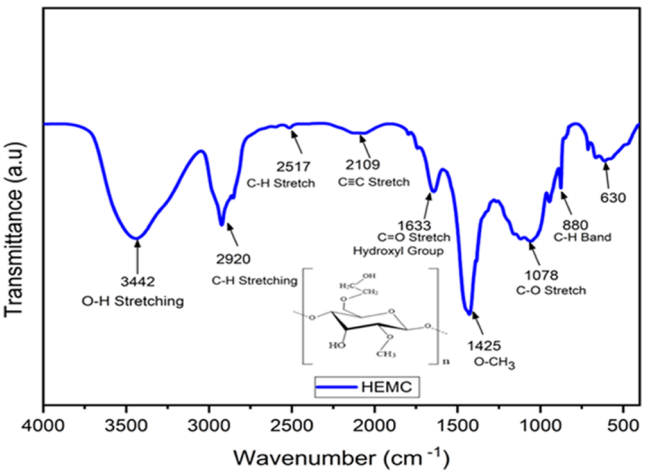

Figure 2. FTIR spectra of HEMC polymer and chemical structure.

caused by the C–H stretch of the aliphatic group is observed, which is generally related to crystalline cellulose.[42,43] The weak peak noticed at 2517 cm^{-1} is associated with the sp^3 C–H stretching, which occurs due to vibration of the cellulose unit. The weak band observed at 2109 cm^{-1} is attributed to the C ≡ C stretch of the alkyne group. A medium-intensity band detected at 1633 cm^{-1} corresponds to the C═O stretch of the secondary hydroxyl group.[44] The strong transmittance peak at 1425 cm^{-1} relates to O–CH$_3$ in the methoxy composite, indicating the amorphous crystalline structure in cellulose ether.[45] The transmittance band observed at 1078 cm^{-1} is attributed to the C–O stretching, indicating β-glycosidic characteristics that bind glucose components within cellulose.[46] The bands observed at 630 and 880 cm^{-1} regions correspond to the C–H band located in fingerprint territory, representing the characteristics of the alkyl and methyl groups, respectively.

The FTIR spectra of unmodified and modified polymer composites are shown in Figure 3. The characteristic bands of organic carbonate (PC and DEC) association were detected in the C–H band, O–CH$_3$ band, and C═O stretch regions. It was observed that weak disubstituted symmetry peaks at 882 cm^{-1} in the C–H band region of the HEMC polymer shifted to 772 cm^{-1} in the modified polymer. The new peak observed in the modified polymer is attributed to the disubstituted

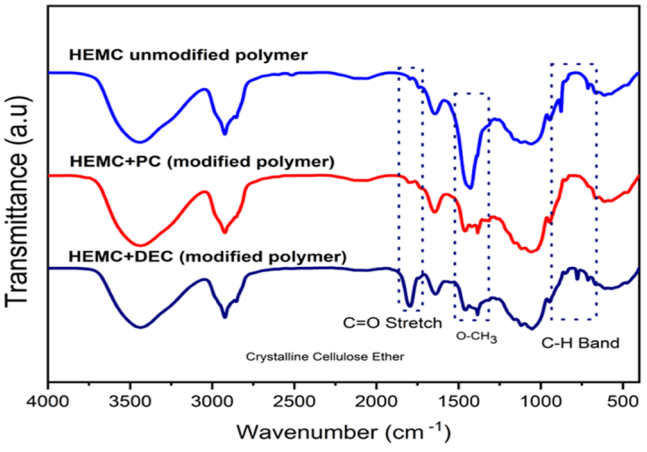

Figure 3. FTIR spectra of native HEMC, HEMC with PC (modified sample), and HEMC with DEC (modified sample).

https://doi.org/10.1021/acsomega.3c02974
ACS Omega 2023, 8, 25453–25466

structural isomer in the alkyl structure. Similarly, the strong transmittance peak at 1435 cm^{-1} shifted to a weak transmittance peak as detected in the O−CH_3 region of the modified polymer samples, indicating a new attachment on the native polymer. A new transmittance peak at 1804 cm^{-1} was found in the C═O stretch region of the modified sample, which ratified the modification and substitution of PC and DEC on the native HEMC polymer surface.

3.2. Structural H-NMR Analysis. The H-NMR spectra of native HEMC and modified composites are shown in Figure 4. The spectra of all samples show chemical shifts between δ (ppm) = 2.3−1.0 attributed to the methyl group (−CH_3), 4.8−3.2 assigned to the ethylene group (−CH_2−CH_2−OH) of the hydroxyethyl cellulose (HEMC) backbone and 7.4−7.1 to the free hydroxy group (−OH) of the anhydro-glucose unit (AGU).[47] In comparison, it can be clearly seen in Figure 4a,b that the high-intensity peaks at 3.4 to 3.2 ppm in the native HEMC polymer sample shift to a weak-intensity peak in modified HEMC with PC sample due to the C−H stretch of the aliphatic group. Additionally, the moderate-intensity peak at chemical shift (δ) 4.5 and 4.9 ppm of HEMC polymer is transferred into a high-intensity peak. A new peak at 4.2 ppm is detected in the modified sample, attributed to the addition of the carboxyl functional group of PC on free hydroxyl of the ethyl group at OH-6. Next, three new peaks of moderate intensity are generated between the 7.4 and 8.1 ppm chemical shift region of the DEC-modified HEMC sample, which was not observed in the native sample, as shown in Figure 4c. The appearance of these new peaks on the modified sample represents the grafting of the carboxyl group of organic carbonates onto the free hydroxy group (−OH) of AGU at position 3-OH assigned to the stretching of C═O. The possible molecular structures after modifications are also shown in Figure 4. The appearance of new peaks in the spectra represents the substitution of PC on the ethyl group and DEC on the AGU and confirms the modification of HEMC.

3.3. Crystalline Structure XRD Evaluation. The XRD profiles of both HEMC modified and unmodified samples revealed peaks at $2\theta \approx 20.5$, 27.6, and 32° regions, as shown in Figure 5. The investigated samples' diffractograms profile showed semicrystalline characteristics, which have crystalline peaks and an amorphous broad hump.[48] The sharp peak at the 32° region describes the semicrystalline nature of HEMC. It was observed that the shape of the modified sample peaks remained unchanged. However, the intensity was slightly reduced and sifted to 31.6° in DEC-modified polymer samples, as observed in Figure 5b. The fundamental peak at 2θ = 20.5° became broader in the modified samples, indicating less crystallinity and more amorphous character. In contrast, the unmodified HEMC sample exhibited a sharper peak in the 32° region, indicating a higher crystallinity-to-amorphous ratio. The diffraction patterns of the modified composites showed a reduction in the crystalline structure, indicating conversion to the amorphous phase. Therefore, the modified HEMC polymer has excellent solubility, as lower crystallinity is associated with higher solubility.[49]

The crystallinity index (CrI) of polymer composites was calculated through the deconvolution method described in eq 1. The CrI of the native HEMC polymer was 54.8%. During the modification process, alkaline replaced hemicellulose, which decreased the crystallinity index.[50] This was also confirmed by the absence of hemicellulose characteristic peaks

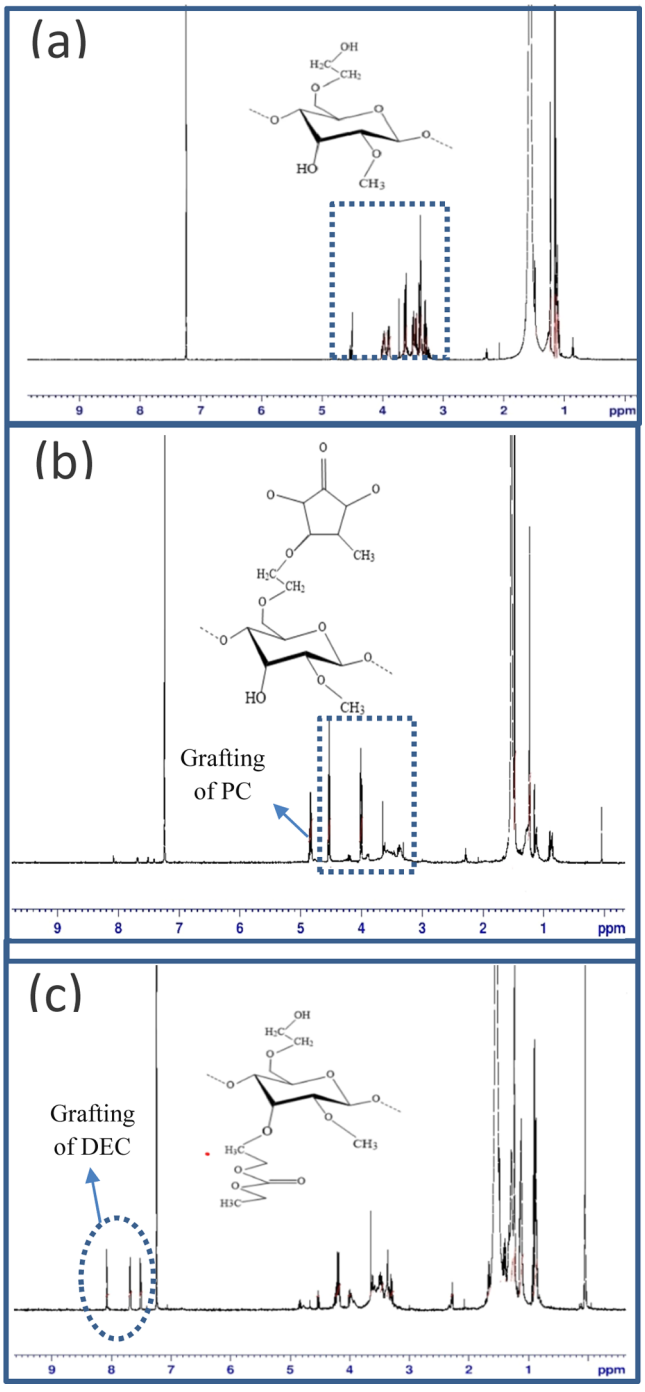

Figure 4. H-NMR spectrum of all samples for structural analysis: (a) native HEMC polymer, (b) modified HEMC with PC, and (c) modified HEMC with DEC.

in the FTIR results, indicating its significant removal after modification. As cellulose is semicrystalline in nature, the addition of PC led to a reduction in the crystallinity index to 52.3%, approaching more amorphous characteristics. During the DEC modification process, the cellulose molecules were cured in an ethylene medium, causing swelling in cellulose particles that exerted pressure on the crystalline part of the molecules and distorted them favorably. The dissociation and distortion of the crystalline part in cellulose molecules further reduced the CrI up to 49.6% for the (HEMC with DEC) modified sample.[51,52]

https://doi.org/10.1021/acsomega.3c02974
ACS Omega 2023, 8, 25453−25466

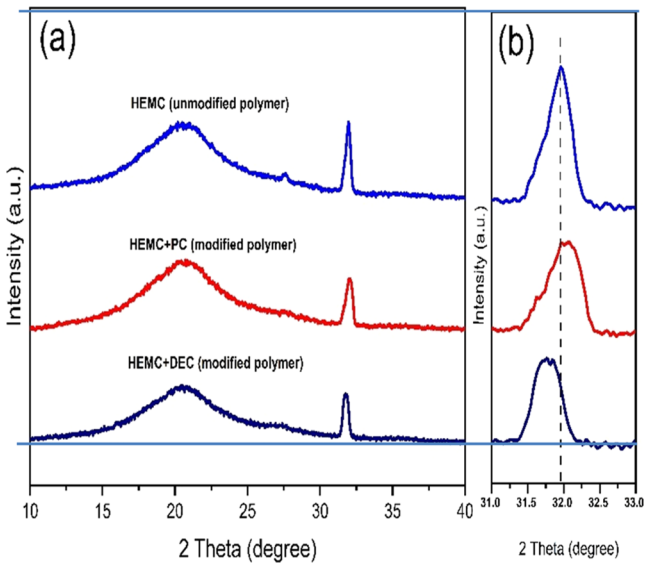

Figure 5. Diffractograms of (a) unmodified and modified samples, and (b) enlarged XRD profile of all samples.

3.4. Morphology SEM Analysis. The SEM images in Figure 6a−f show morphological differences between unmodified and modified composites at 5 and 50 μm. The HEMC polymer has a long, tortuous, and rod-like shape of various lengths with a rough surface. Considerable morphological changes occurred on the surface of the HEMC polymer due to the inclusion of PC and DEC (organic carbonates). A layer of organic carbonate on the surface of the native polymer indicates that the HEMC native polymer was grafted, as observed in Figure 6a−c. Further, the cloudy layer on the polymer surface showed an amorphous phase.

3.5. Thermogravimetric Analysis. The thermogravimetric analysis evaluates the thermal changes in materials after modification and determines the thermal stability of polymer samples. Figure 7 shows the thermal degradation of unmodified HEMC polymer. The initial weight (wt) loss of approximately 4% starts at 40 °C and ends at 80 °C. The wt loss at this early and slow pyrolysis curve is related to the volatilization and vaporization of water. In the continuous heating run, additional mass loss was observed. However, this time, a three-stage process was involved in the thermal decomposition of cellulose ether. In the first stage, 8.5% weight loss in the sample was observed between 80 and 200 °C and was associated with the degradation of cellulose ether.

The second wt loss was in the temperature range of 200−375 °C with a maximum weight loss of 70.5%. In the third stage, a weight loss of 11% was observed up to 435 °C. The cumulative loss of 81.2% was attributed to depolymerization and the presence of COO groups, which were decarboxylated at that temperature.[1] The degradation temperature in the modified polymer samples was slightly shifted toward higher values. First step thermal degradation temperature shifted to 89 °C with 3.3% wt loss for PC-modified polymer sample and to 95 °C with 2.5% wt loss for the DEC-modified polymer sample, as shown in Figures 8 and 9. This low weight loss of modified polymer composites was due to the addition of carbonates that creates strong interaction with native polymer.[34]

Similarly, the second step degradation temperature of the modified polymer samples was shifted to 212 and 226 °C for PC and DEC modification, respectively. The remaining residue at 500 °C for all samples verified that modified samples have 3 and 10 wt % residues, respectively, while HEMC native polymer completely decomposed at a temperature of 496 °C, indicating that the modified polymer samples are more stable than the native polymer.

3.6. DSC Thermal Analysis. Figure 10 shows the DSC thermogram of HEMC and modified samples from 40 to 250 °C. The DSC curves of all polymeric samples have only one distinct endothermic change in the given temperature range. The detected heat flow signal showed that the phase morphology of all samples was homogeneous. The endothermic heat flow from 50 to 120 °C represents water vaporization in polymer samples. The maximum vaporization temperature of the native HEMC sample was 83 °C, which was attributed to hydrophilic substances that retain moisture in cellulose. Moreover, the addition of PC and DEC shifted the endothermic peak toward a higher temperature, as observed in Figure 10. The vaporization temperature shifted to 90 °C for PC-modified and 101 °C for DEC-modified samples. The increase in vaporization temperature for modified polymer composites was due to the rearrangement of the polymeric molecular chain and an increase in the amorphous component and increased cross-linking density because of organic solvents.[53,54] The DSC result and vaporization temperature increase showed that the addition of organic carbonates increases thermal stability.

3.7. ζ-Potential Measurement and Analysis. The ζ-potential magnitude indicates the polymer solution's physical stability in the aqueous system. The stability of the material is dependent on the ζ-potential value. Polymer solutions with high ζ-potential values are considered stable, while those with low values are weak and unstable. The ζ-potential of native and modified HEMC polymeric solutions was determined and is presented in Figure 11. The ζ-potential magnitude of the HEMC polymer sample was −12 mV. The low value of HEMC polymer represents weak electrostatic colloidal stability of suspension in electrolyte behavior.[55] Whereas the ζ-potential magnitude of grafted polymer samples was −37 mV for PC and −44.5 mV for DEC. The particles tend to repel each other in an aqueous solution and prevent the fluctuation of particles, which leads to the high colloidal stability of modified polymers.[56] Further, more negative-charged reactive carbonate could be absorbed onto the polymer-modified composite than the unmodified one.[35] Hence, ζ-potential measurement shows strong cross-linking interactions of HEMC with organic solvents indicating better dispersion stability.

3.8. Molecular Weight Measurement and Analysis. The molecular weight of modified polymer solutions was determined using the Mark−Houwink−Sakurada (MHS) equation. However, Houwink's coefficient and constant (a and K) for HEMC polymer were unavailable. Therefore, it was necessary to determine the coefficient and constant for the HEMC polymer. First, the relative viscometry method determined the intrinsic viscosity of known molecular weight polymer solutions. The viscometry results and other relevant viscosities determined using eqs 3−8 are provided in Table 1.

Extrapolation of reduced viscosity up to zero concentration provides the intrinsic viscosity of the defined molecular weight of the HEMC solution, as shown in Figure 12. The value of a and K for HEMC polymer was determined by graphical

https://doi.org/10.1021/acsomega.3c02974
ACS Omega 2023, 8, 25453−25466

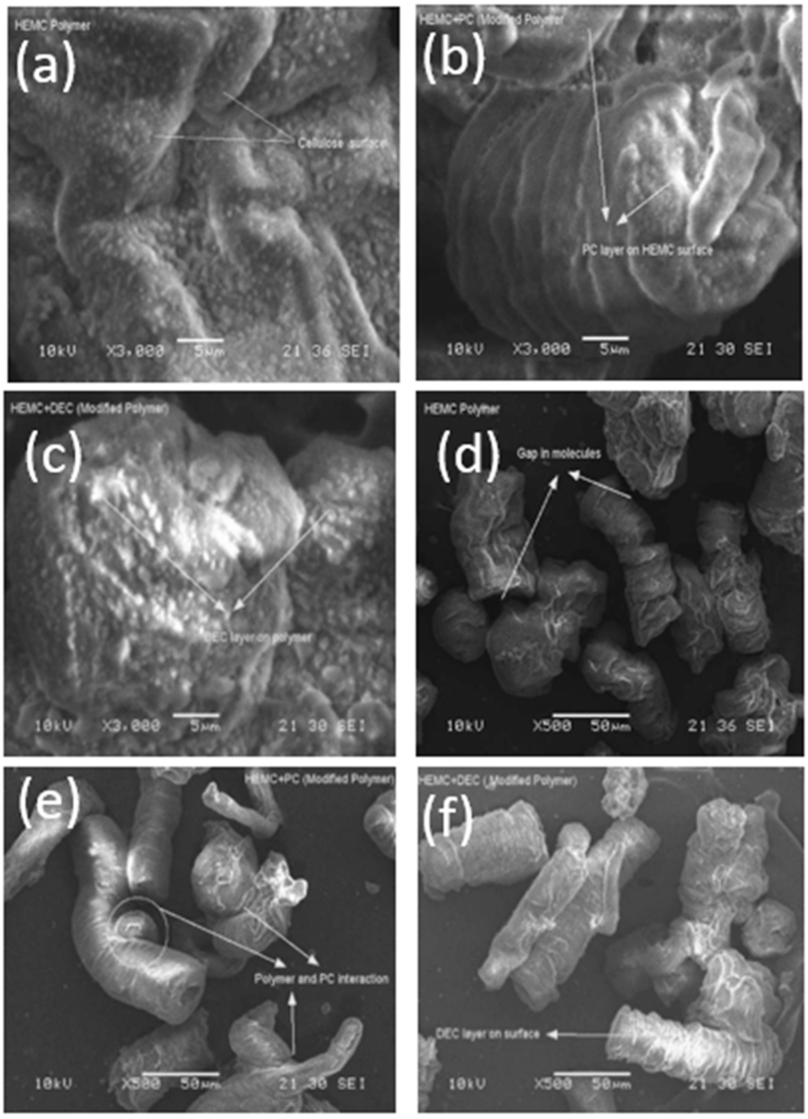

Figure 6. Scanning electron microscopic images of (a) native HEMC at 5 μm, (b) HEMC + PC-modified composite at 5 μm, (c) HEMC + DEC-modified composite at 5 μm, (d) native HEMC at 50 μm, (e) HEMC + PC-modified composite at 50 μm, and (f) HEMC + DEC-modified composite at 50 μm.

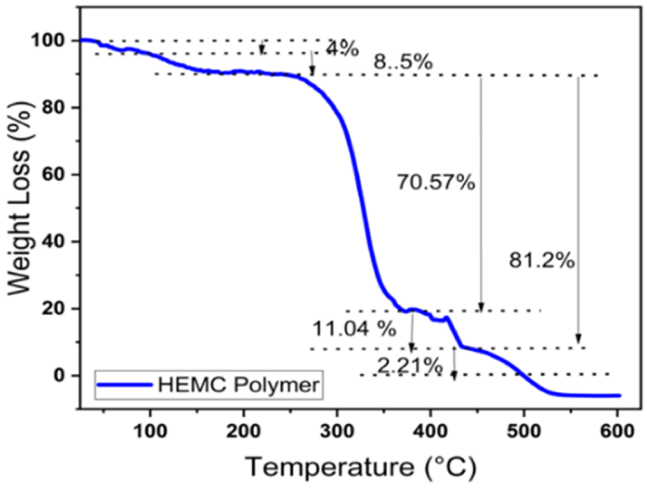

Figure 7. TGA curve of the native HEMC sample.

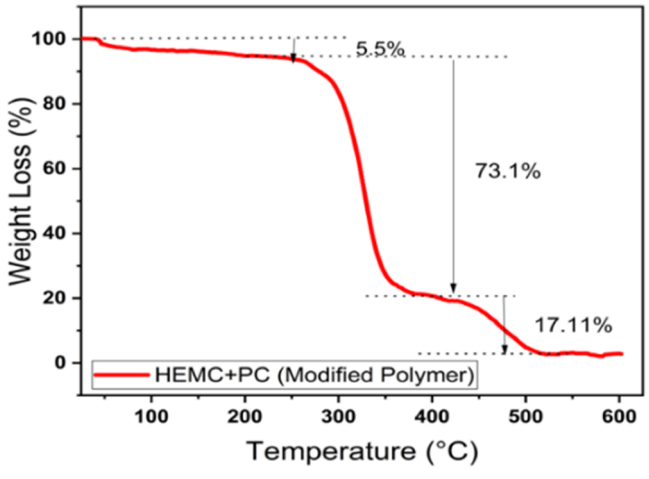

Figure 8. TGA curve of (HEMC with PC) modified sample.

representation using the following equation derived from the MHS equation

https://doi.org/10.1021/acsomega.3c02974
ACS Omega 2023, 8, 25453−25466

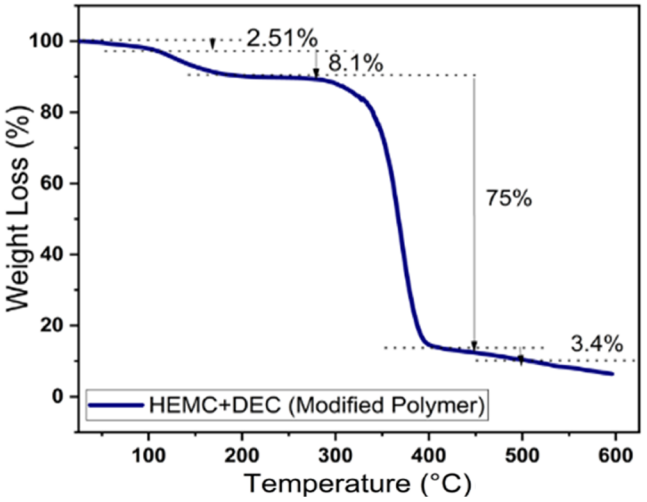

Figure 9. TGA curve of the (HEMC with DEC) modified sample.

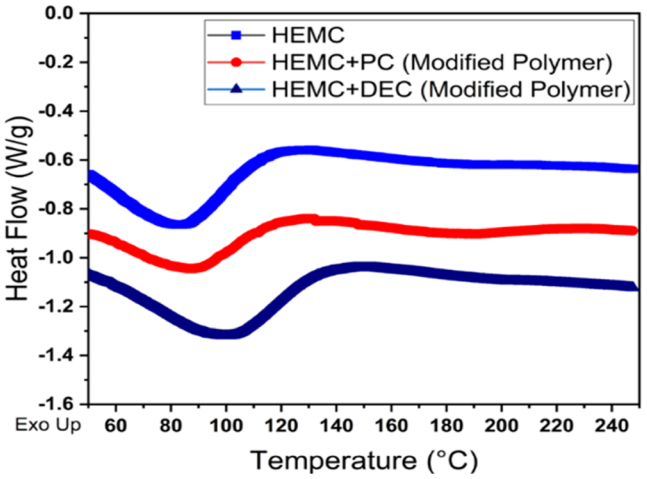

Figure 10. DSC curve of native HEMC, HEMC with PC (modified polymer), and HEMC with DEC (modified polymer).

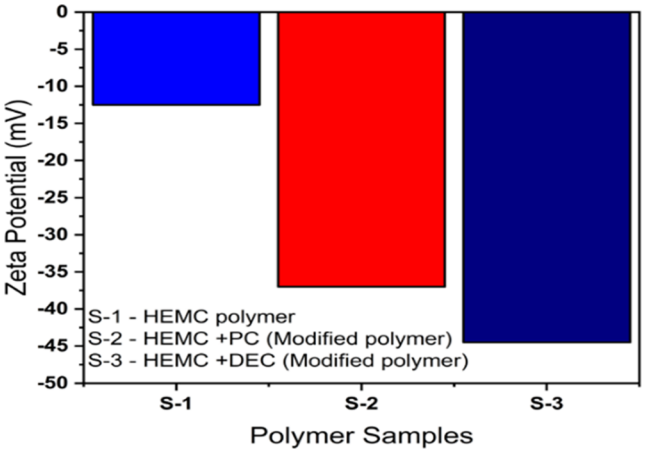

Figure 11. ζ-potential of the unmodified and modified polymer solution.

$$\log[\eta] = \log K + a \log[M_w] \quad (9)$$

In the above equation, a log−log graph was drawn between intrinsic viscosity and molecular weight. The slope of the straight line represents the constant value "*a*," and its intercept

Table 1. Viscometry Results of HEMC Solution by Changing Molecular Weight at 25 °C

molecular weight (M_w)	solution concentration (C)	flow time (t_s)	relative viscosity (η_r)	specific viscosity (η_{sp})	reduced viscosity (η_{red})
40,000	0.002	26.96	1.272	0.272	135.849
	0.003	30.54	1.441	0.441	146.855
	0.004	34.68	1.636	0.636	158.962
	0.005	40.06	1.89	0.89	177.924
52,000	0.002	28.19	1.33	0.33	164.858
	0.003	32.52	1.534	0.534	177.987
	0.004	36.71	1.732	0.732	182.901
	0.005	42.18	1.99	0.99	197.924
60,000	0.002	29.04	1.37	0.37	184.905
	0.003	33.79	1.594	0.594	197.955
	0.004	39.34	1.856	0.856	213.915
	0.005	45.57	2.15	1.15	229.902
75,000	0.002	30.61	1.444	0.444	221.933
	0.003	36.40	1.717	0.717	238.993
	0.004	42.56	2.008	1.008	251.886
	0.005	49.71	2.345	1.345	268.962
80,000	0.002	31.82	1.524	0.524	250.474
	0.003	38.43	1.813	0.813	270.911
	0.004	45.79	2.16	1.16	289.976
	0.005	54.69	2.58	1.58	315.943
90,000	0.002	33.01	1.557	0.557	278.537
	0.003	40.34	1.903	0.903	300.943
	0.004	47.91	2.26	1.26	314.976
	0.005	57.76	2.725	1.725	344.906

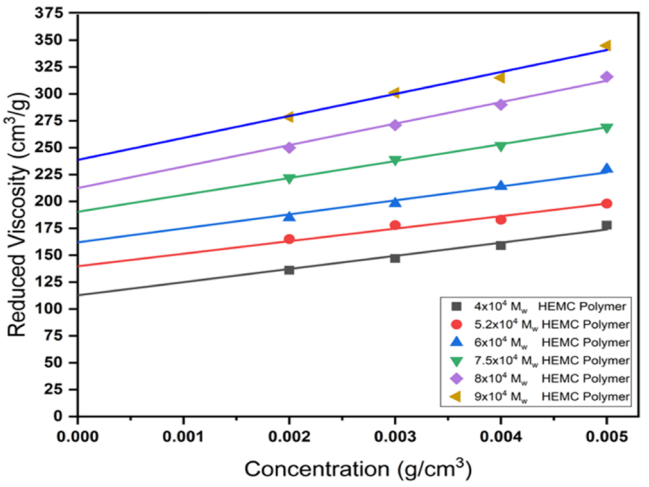

Figure 12. Concentration vs reduced viscosity profiles of different-molecular weight HEMC polymer dissolved in water at 25 °C.

provides the value of "log k," as shown in Figure 13. The value of "*a*" was determined to be 0.89, and the value of "K" was found to be 0.00927 (9.27×10^{-3}) for HEMC polymer in water solvent at 25 °C. The Mark−Houwink exponent provides information regarding the polymer chain configuration in the solvent environment. As the value of "a" was 0.89, the polymer is a random coil in a good solvent.[37]

The viscometry experimental results and viscosity measurement using eqs 3−8 for both modified samples are provided in Tables 2 and 3.

The elapsed flow time of solvent (t) was 21.2 s. The intercept of reduced viscosity and inherent viscosity at zero concentration provides the intrinsic viscosity of the solution.

https://doi.org/10.1021/acsomega.3c02974
ACS Omega 2023, 8, 25453−25466

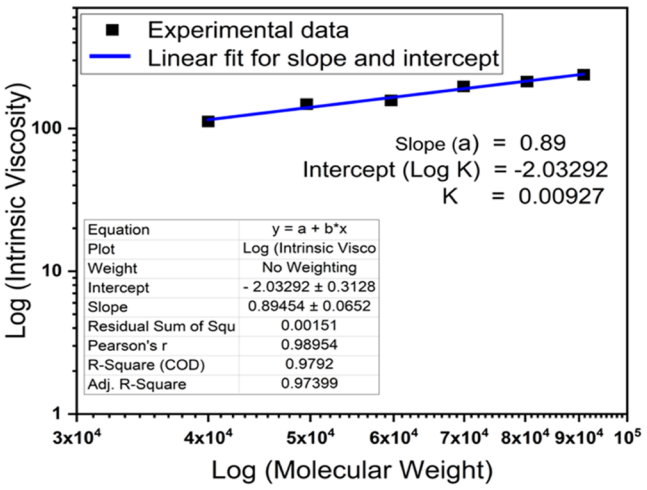

Figure 13. Log molecular weight vs log reduced intrinsic viscosity profiles of HEMC polymers.

Table 2. Viscometry Results of PC-Modified HEMC Solution in Water at 25 °C

polymer concentration (C)	t_s	η_r	η_{inh}	η_{sp}	η_{red}
0.002	33.45	1.568	228.049	0.568	289
0.003	41.52	1.958	224.059	0.958	319.5
0.004	49.69	2.343	212.951	1.343	335.97
0.005	59.89	2.825	207.708	1.825	365.02

Table 3. Viscometry Results of DEC-Modified HEMC Solution in Water at 25 °C

polymer concentration (C)	t_s	η_r	η_{inh}	η_{sp}	η_{red}
0.002	34.13	1.617	238.117	0.612	305.25
0.003	41.55	1.962	224.314	0.964	320.07
0.004	50.37	2.376	216.354	1.376	344.68
0.005	60.42	2.851	209.463	1.859	370.14

The intrinsic viscosity of the modified (HEMC with PC) polymer solution was 245 and 260 cm^3/g for the (HEMC with DEC) modified polymer solution, as shown in Figure 14a,b. The molecular weight of the HEMC polymer was 9 × 10^4 g/mol as provided by the supplier.

The molecular weight of modified polymer samples was determined using MHS eq 2 with a = 0.89 and K = 0.00927 for HEMC polymer in water solvent at 25 °C.

$$[\eta] = 9.27 \times 10^{-3} [M^{0.89}] \quad (10)$$

The molecular weight of the PC-modified sample was 9.3 × 10^4 g/mol and 9.9 × 10^4 g/mole for the DEC-modified sample. The obtained values showed that the modified samples have an increased molecular weight due to the inclusion of PC and DEC in the cellulose ether polymer.

3.9. Rheology Measurement and Impact of Organic Carbonate on Viscosity of the Polymer Solution. The rheological properties of both native and modified samples were examined through shear rate sweep and temperature sweep analyses. Initially, the solubility and hydration rates of the polymer solutions were determined at a constant shear rate of 10 (1/s) and room temperature. The hydration rate of modified samples was observed to be like the unmodified HEMC, as shown in Figure 15. The modified polymers

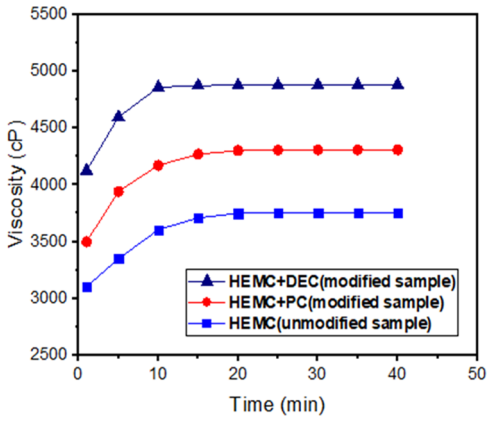

Figure 15. Hydration rate of polymer solutions at room temperature.

exhibited comparable solubility and hydration rates to the unmodified HEMC native solution, while the viscosity of the soluble modified products was notably higher than that of the unmodified sample. The DEC-modified sample hydrated and reached maximum viscosity earlier than the PC-modified and native HEMC solutions. The DEC-modified composite exhibited greater and higher viscosity compared to the other

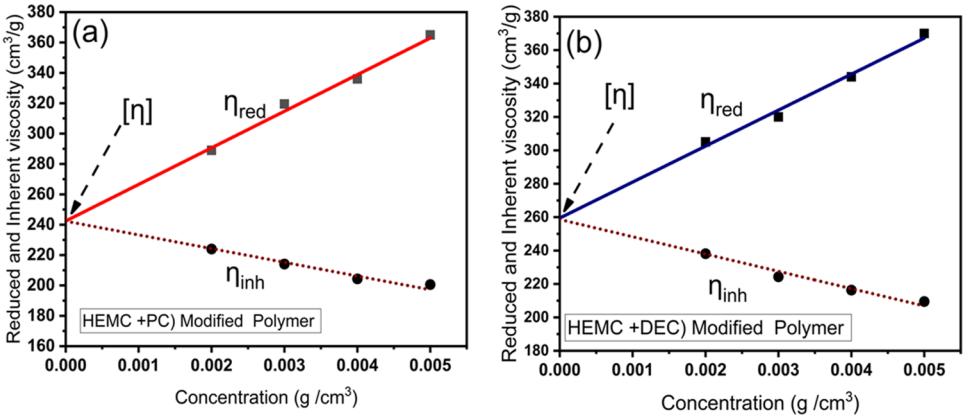

Figure 14. Reduced and inherent viscosity of (a) HEMC + PC (modified polymer) and (b) HEMC + PC (modified polymer) by changing the concentration in water at 25 °C.

https://doi.org/10.1021/acsomega.3c02974
ACS Omega 2023, 8, 25453−25466

samples, which can be attributed to the higher molecular weight of the modified samples.

To conduct a temperature sweep analysis, the viscosity of solutions was determined at a constant shear rate of 10 (1/s) while systematically increasing the temperature. The viscosity of the polymer solution was found to be affected by changes in temperature, as a consistent decrease in viscosity was observed in Figure 16. As the temperature increases, the

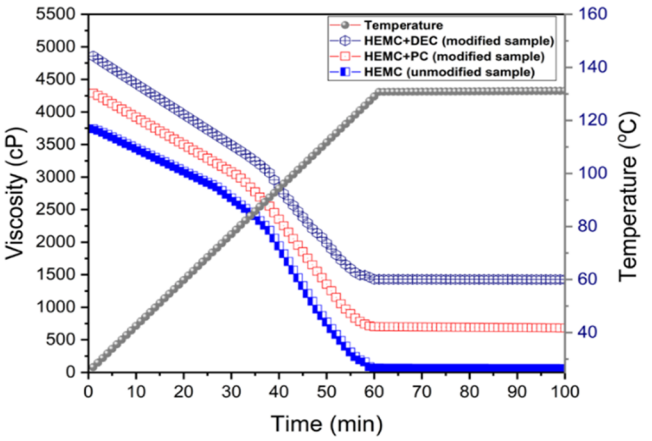

Figure 16. Viscosity profile w.r.t time by changing the temperature of unmodified and modified HEMC solution at a constant shear rate.

viscosity of the HEMC solution decreases gradually. However, beyond 80 °C, the rate of viscosity reduction significantly accelerates. The solution reached its maximum reduction in viscosity at 115 °C. DSC analysis confirmed that the evaporation temperature of HEMC was 83 °C at which point the polymer began to dehydrate. Consequently, a significant change in viscosity was observed above the evaporation temperature. The sample exhibited a minimum viscosity of 60 cP up to 130 °C. Conversely, the viscosity of the modified samples was higher than that of the native solution at their respective temperatures. The PC-modified solution exhibited a viscosity of 702 cP, while the DEC-modified solution exhibited a viscosity of 1432 cP at 130 °C, respectively.

The rotational viscosity of the polymer samples was also determined to evaluate the shear rate behavior. Figure 17a represents the viscosity profile of 01 weight percent concentration polymer solution w.r.t shear rate at 30 °C. The data showed significant shear-thinning behavior (non-Newtonian), where viscosity reduction was observed due to the partial alignment and uncoiling of polymer chains in high-shear-rate regions and due to the orientation of the microstructures in the direction of given deformation. In petroleum industry applications, shear-thinning behavior is an ideal scenario for various processes such as drill cutting transport and suspension in drilling fluids, pumping cement slurry, and polymer flooding for EOR applications.[57,58]

The viscosity of the solutions was high at low shear rates due to the high molecular weight of the polymer and strong interaction forces between the molecules in the solution. The shear viscosity of the modified HEMC was greater than that of the unmodified polymer solution due to the higher molecular weight. The mechanical properties of the modified polymers increased due to the longer molecular chains and the interaction between the chains. The shear viscosity of the polymer solutions was also determined at 90 °C to evaluate the shear and thermal behavior simultaneously. It was observed that the modified polymer solutions had a higher viscosity than the native HEMC polymer solution, as shown in Figure 17b. The presence of PC and DEC improves intermolecular interactions and creates cross-linking in polymer particles, which enhances viscosity. A reduced and low viscosity was observed at an elevated temperature of 90 °C compared to 30 °C. The change and decrease in viscosity can be attributed to the transformation of the molecule from a rod-like structure (ordered) to a more flexible structure (disordered), and a decrease in the rigidity of the glucan chain with an increasing temperature.[59]

3.10. Chemical Reaction and Proposed Mechanism of Modification. HEMC is a random coil-type structure in aqueous media and hydrophilic in nature, which completely dissolves in aqueous water. Meanwhile, PC and DEC are organic carbonates used as reactive diluents and trans-esterification agents in polymer synthesis. Modification of cellulose ether takes place via a homogeneous route in which cellulose dissolves in organic carbonate, degrading the

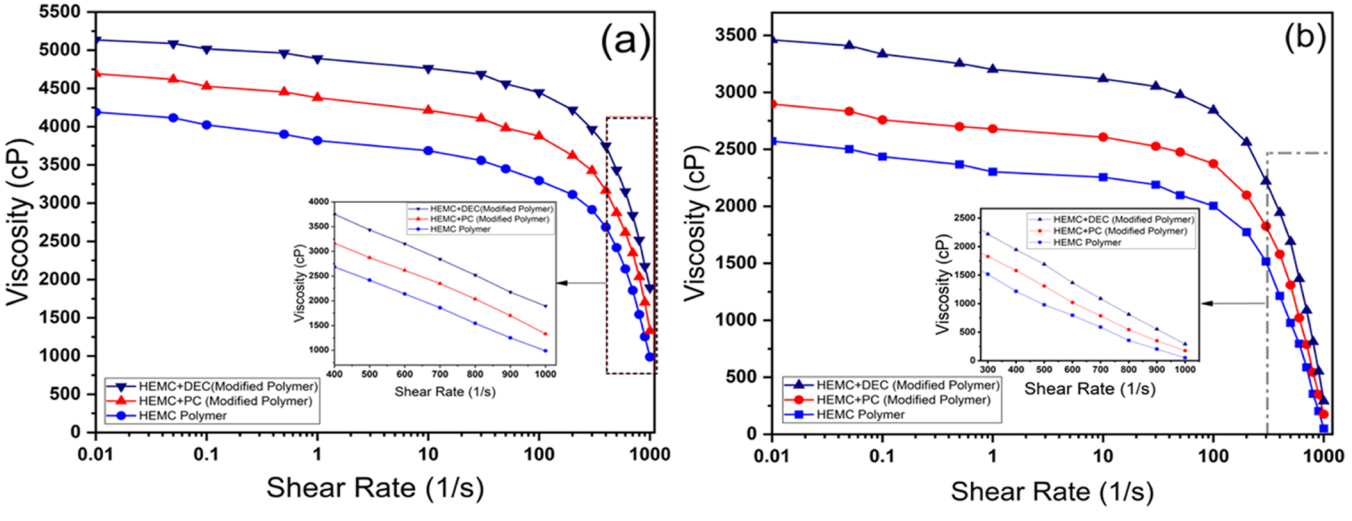

Figure 17. Rotational viscosity of 01 wt % polymer solutions w.r.t shear rate (a) at 30 °C and (b) at 90 °C.

https://doi.org/10.1021/acsomega.3c02974
ACS Omega 2023, 8, 25453−25466

supramolecular structure and improving the accessibility of hydroxyl groups for the reaction.[60] During conjugation, the cellulose fibers collapse into rod-like structures (also observed in SEM analysis) where the amorphous region of cellulose ether is more sensitive to attack by solvent molecule for the chemical reaction. The modification process involves carbonation and etherification, achieved through a homogeneous alkoxy carbonylation process of cellulose ether using propylene carbonate and diethyl carbonate solvents.[33] In dry and wet methods, no catalyst was used for modification. Therefore, the reaction between both products commenced due to thermodynamic factors and heating of the sample.[61] The reaction of organic carbonates with cellulose functional groups occurred due to the availability of sugar rings and free OH groups in cellulose ether. In the HEMC structure, one free hydroxyl group (OH-3) on AGU and another −OH on the ethyl group (OH-6) were available to react with organic carbonates, as shown in Figure 18.

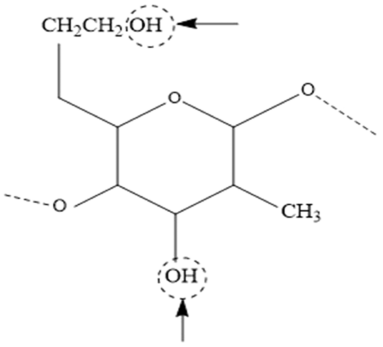

Figure 18. Reaction sites for organic carbonate on the monomer unit of HEMC containing pyranose ring.

The chemical reaction of organic carbonate with cellulose ether is depicted in Schemes 2 and 3. The acyclic carbonate DEC interacts with the free hydroxyl group (OH-3) and PC (cyclic carbonate) attaches to the free hydroxy of the ether group through etherification and carbonation modification processes. It appears that a double reaction occurs simultaneously between the monomer ring of the cellulose functional group and molecule of organic carbonate molecule in the form of inter- and intra-annular interaction, as shown in Figure 19.[33] In the reaction process, hydroxyethylation of cellulose typically enhances the solubility, while inter- and intra-annular intrachain formation increases the molecular weight of the polymer, as shown in Figure 20. Thus, the intrachain formation between the hydroxyl group and carbonate increases the molecular weight, solubility, and thermal stability.

4. CONCLUSIONS

Based on the extensive and integrated study of cellulose ether modification by organic solvents, it is concluded that the cellulose ether structure was successfully modified and confirmed through FTIR and H-NMR structural analyses. The modification introduces new functional groups to the native polymer without altering its morphology. The modification decreases the crystallinity of HEMC and improves the solubility in aqueous solutions as confirmed by XRD patterns of morphology analysis. The addition of organic carbonate significantly increased the vaporization temperature by 90 °C (for PC) and 101 °C (for DEC) and raised the decomposition temperature above 500 °C, indicating higher stability compared to unmodified composites. The ζ-potential measurement confirms the enhanced stability of grafted composites. Organic carbonates have a remarkable impact on the molecular weight of cellulose ether. The addition of organic carbonate enhances the molecular weight from 9×10^4 to 9.3×10^4 and 9.9×10^4 g/mol for PC- and DEC-containing modified samples, respectively, improving its impact on shear and thermal viscosity. A rheological investigation focusing on viscosity provides a comprehensive understanding of the stability and activation of composites modified with carbonate. Organic carbonates acted as transesterification agents, linked through carbonation and etherification modification that activated on heat and improved the thermal stability of cellulose ether. Hence, the thermal and rheological properties of modified polymer samples were significantly improved by adding a small aspect ratio of organic carbonate in cellulose ether. The new cellulose ether that has been developed using organic carbonate possesses several multifunctional properties. It exhibits an increased thermal degradation temperature and improved stability, solubility, hydration rate, and viscosity under shear rate and high-temperature conditions. The modified polymer with DEC is more effective than PC modified in all aspects of characterization due to its linkage on the anhydro-glucose unit of cellulose ether, as concluded from the study.

The findings of this study provide in-depth knowledge to understand the behavior and to synergize the properties of modified cellulose ether, which can be utilized to create tailored materials for industrial applications. Further, research should focus on determining the API properties of these modified composites, as this would have a positive impact on drilling/cementing ventures and EOR applications positively. These findings can potentially drive innovation in polymer modification and contribute to the development of more efficient and effective materials for petroleum and other various industries.

Scheme 2. Chemical Reaction of Cellulose Ether (HEMC) with PC for Modification

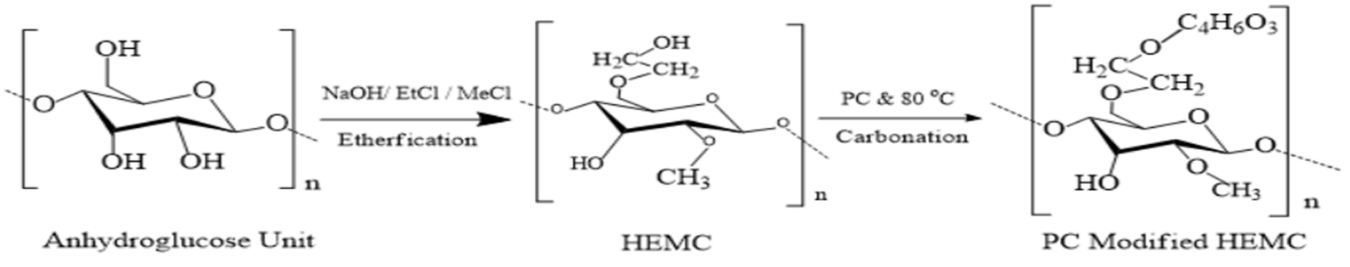

https://doi.org/10.1021/acsomega.3c02974
ACS Omega 2023, 8, 25453−25466

Scheme 3. Chemical Reaction of Cellulose Ether (HEMC) with DEC for Modification

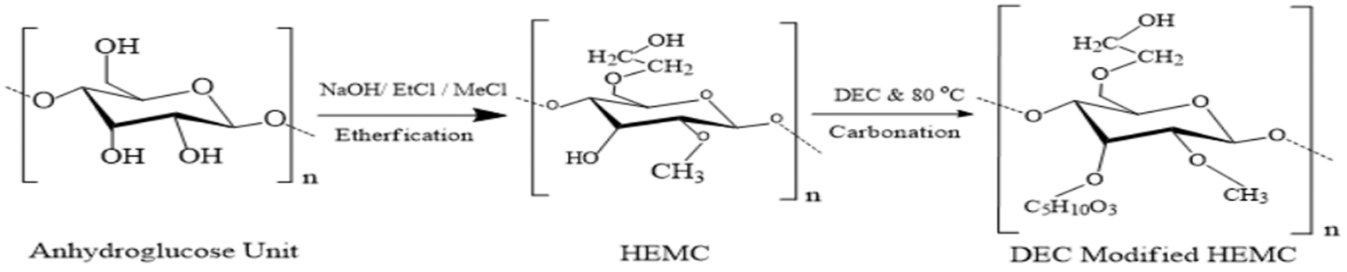

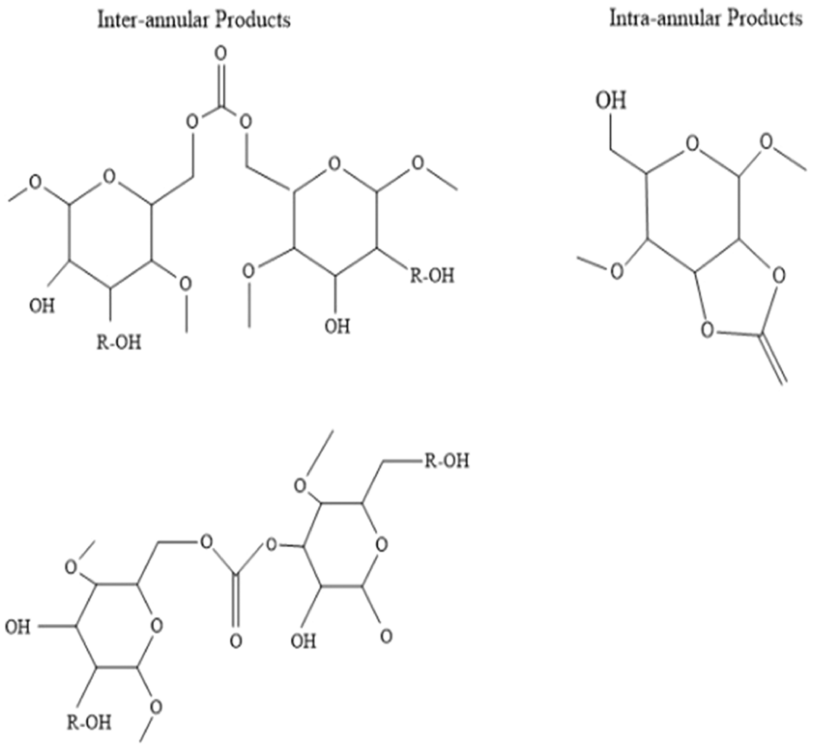

Figure 19. Possible inter- and intra-annular product formation through the reaction between organic carbonate and hexose units of HEMC.

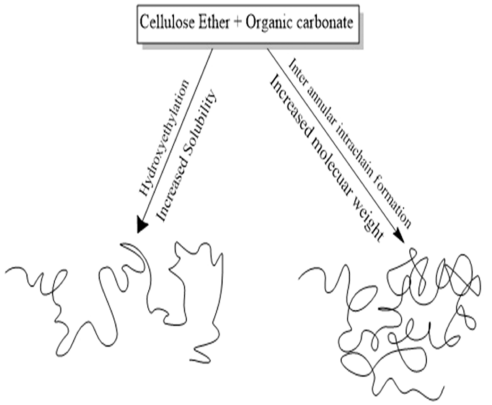

Figure 20. Schematic representation of potential product formation for the organic carbonate reaction with HEMC.

AUTHOR INFORMATION

Corresponding Author

Ghulam Abbas − *Institute of Petroleum & Natural Gas Engineering, Mehran University of Engineering & Technology, Jamshoro 76062 Sindh, Pakistan;* orcid.org/0009-0008-6625-9249; Phone: +92-3009678879; Email: engr_abbas@muetkhp.edu.pk

Authors

Abdul Haque Tunio − *Institute of Petroleum & Natural Gas Engineering, Mehran University of Engineering & Technology, Jamshoro 76062 Sindh, Pakistan*

Khalil Rehman Memon − *Institute of Petroleum & Natural Gas Engineering, Mehran University of Engineering & Technology, Jamshoro 76062 Sindh, Pakistan*

Aftab Ahmed Mahesar − *Institute of Petroleum & Natural Gas Engineering, Mehran University of Engineering & Technology, Jamshoro 76062 Sindh, Pakistan*

Faisal Hussain Memon − *Department of Petroleum & Natural Gas Engineering, Mehran University of Engineering & Technology, Khairpur Mirs 66020 Sindh, Pakistan;* orcid.org/0009-0008-4024-3185

Ghazanfer Raza Abbasi − *School of Engineering, Edith Cowan University, Joondalup, Western Australia 6027, Australia*

Complete contact information is available at: https://pubs.acs.org/10.1021/acsomega.3c02974

https://doi.org/10.1021/acsomega.3c02974
ACS Omega 2023, 8, 25453−25466

Notes

The authors declare no competing financial interest.

■ ACKNOWLEDGMENTS

The authors would like to gratefully acknowledge Mehran University of Engineering and Technology (MUET), Jamshoro, Sindh, Pakistan, for their financial and technical support of this research.

■ REFERENCES

(1) Owi, W. T.; Lin, O. H.; Sam, S. T.; Chia, C. H.; Zakaria, S.; Mohaiyiddin, M. S.; Villagracia, A. R.; Santos, G. N.; Akil, H. M. Comparative Study of Microcelluloses Isolated from Two Different Biomasses with Commercial Cellulose. *BioResources* **2016**, *11*, 3453−3465.

(2) Tsioptsias, C.; Stefopoulos, A.; Kokkinomalis, I.; Papadopoulou, L.; Panayiotou, C. Development of Micro- and Nano-Porous Composite Materials by Processing Cellulose with Ionic Liquids and Supercritical CO2. *Green Chem.* **2008**, *10*, 965−997.

(3) Zheng, X.; Huang, F.; Chen, L.; Huang, L.; Cao, S.; Ma, X. Preparation of Transparent Film via Cellulose Regeneration: Correlations between Ionic Liquid and Film Properties. *Carbohydr. Polym.* **2019**, *203*, 214−218.

(4) Whistler R, B. J. *Industrial Gums: Polysaccharidesand their Derivatives*, 3rd ed.; Academic Press Limited: London, 1993.

(5) Abbas, G.; Irawan, S.; Kumar, S.; Memon, K. R.; Khalwar, S. A. Characteristics of Oil Well Cement Slurry Using Hydroxypropylmethylcellulose. *J. Appl. Sci.* **2014**, *14*, 1154−1160.

(6) Abbas, G.; Irawan, S.; Memon, K. R.; Khan, J. Application of Cellulose-Based Polymers in Oil Well Cementing. *J. Pet. Explor. Prod. Technol.* **2020**, *10*, 319−325.

(7) Klemm, D.; Philipp, B.; Heinze, T.; Heinze, U.; Wagenknect, W. Comprehensive Cellulose Chemistry. In *Functionalization of Cellulose*; Wiley, 1998; Vol. 2.

(8) Muther, T.; Syed, F. I.; Dahaghi, A. K.; Negahban, S. Socio-Inspired Multi-Cohort Intelligence and Teaching-Learning-Based Optimization for Hydraulic Fracturing Parameters Design in Tight Formations. *J. Energy Resour. Technol.* **2022**, *144*, No. 073201.

(9) Sabzian mellei, A.; Madadizadeh, A.; Riahi, S.; Kaffashi, B. Synergetic Effects of PVP/HEC Polymers on Rheology and Stability of Polymeric Solutions for Enhanced Oil Recovery at Harsh Reservoirs. *J. Pet. Sci. Eng.* **2022**, *215*, No. 110619.

(10) Abbas, G.; Irawan, S.; Kumar, S.; Elrayah, A. A. I. Improving Oil Well Cement Slurry Performance Using Hydroxypropylmethylcellulose Polymer. *Adv. Mater. Res.* **2013**, *787*, 222−227.

(11) Arai, K.; Shikata, T. Hydration/Dehydration Behavior of Cellulose Ethers in Aqueous Solution. *Macromolecules* **2017**, *50*, 5920−5928.

(12) Hamza, A.; Shamlooh, M.; Hussein, I. A.; Nasser, M.; Salehi, S. Polymeric Formulations Used for Loss Circulation Materials and Wellbore Strengthening Applications in Oil and Gas Wells: A Review. *J. Pet. Sci. Eng.* **2019**, *180*, 197−214.

(13) Blazkovz, A.; Hrivikova, J.; Lapcik, L. Viscosity Properties of Aqueous-Solutions of Hydroxyethylcellulose. *Dep. Phys. Chem., Fac., Chem. Pap.* **1990**, *44*, 289−301.

(14) Pope, G. A. Recent Developments and Remaining Challenges of Enhanced Oil Recovery. *J. Pet. Technol.* **2011**, *63*, 65−68.

(15) Glass, J. E.; Soules, Da.; Ahmed, H.; Egland-Jongewaard, S. K.; Fernando, R. H. In *Viscosity Stability of Aqueous Polysaccharide Solutions*, SPE California Regional Meeting; OnePetro, 1983.

(16) Abbas, S.; Donovan, J.; Sanders, A. In *Applicability of Hydroxyethylcellulose Polymers for Chemical EOR*, SPE Enhanced Oil Recovery Conference; OnePetro, 2013.

(17) Arvidson, S. A.; Lott, J. R.; McAllister, J. W.; Zhang, J.; Bates, F. S.; Lodge, T. P.; Sammler, R. L.; Li, Y.; Brackhagen, M. Interplay of Phase Separation and Thermoreversible Gelation in Aqueous Methylcellulose Solutions. *Macromolecules* **2013**, *46*, 300−309.

(18) Kumar, D.; Ganat, T.; Lashari, N.; Ayoub, M. A.; Kalam, S.; Chandio, T. A.; Negash, B. M. Experimental Investigation of GO-HPAM and SiO2-HPAM Composite for CEOR: Rheology, Interfacial Tension Reduction, and Wettability Alteration. *Colloids Surf., A* **2022**, *637*, No. 128189.

(19) Müller, K.; van Opdenbosch, D.; Zollfrank, C. Cellulose Blends with Polylactic Acid or Polyamide 6 from Solution Blending: Microstructure and Polymer Interactions. *Mater. Today Commun.* **2022**, *30*, No. 103074.

(20) Al-Hamairi, A.; AlAmeri, W. Development of a Novel Model to Predict HPAM Viscosity with the Effects of Concentration, Salinity and Divalent Content. *J. Pet. Explor. Prod. Technol.* **2020**, *10*, 1949−1963.

(21) Khan, M. J.; Muther, T.; Aziz, H.; Mubeen-ur-Rehman, M. Investigating the Impact of Injection-Water Salinity and Well Strategies on Water Mobility and Oil Production in an Oil-Wet Reservoir. *Model. Earth Syst. Environ.* **2021**, *7*, 247−260.

(22) Lashari, N.; Ganat, T. Synthesized Graphene Oxide and Fumed Aerosil 380 Dispersion Stability and Characterization with Partially Hydrolyzed Polyacrylamide. *Chin. J. Chem. Eng.* **2021**, *34*, 307−322.

(23) Soares, A. S. F.; Marques, M. R. C.; Calçada, L. A.; Filho, M. N. B.; de Oliveira Petkowicz, C. L. Interaction of Blockers on Drilling Fluids Rheology and Its Effects on Sealing of Fractures and Prevention of Filtrate Invasion. *J. Pet. Sci. Eng.* **2018**, *171*, 260−270.

(24) Adewole, J. K.; Sultan, A. S. A Study on Processing and Chemical Composition of Date Pit Powder for Application in Enhanced Oil Recovery. *Defect Diffus. Forum* **2014**, *353*, 79−83.

(25) Khalil, M.; Mohamed Jan, B. Herschel-Bulkley Rheological Parameters of a Novel Environmentally Friendly Lightweight Biopolymer Drilling Fluid from Xanthan Gum and Starch. *J. Appl. Polym. Sci.* **2012**, *124*, 595−606.

(26) Luheng, Q. The Application of Polymer Mud System in Drilling Engineering. *Procedia Eng.* **2014**, *73*, 230−236.

(27) Ojogbo, E.; Ogunsona, E. O.; Mekonnen, T. H. Chemical and Physical Modifications of Starch for Renewable Polymeric Materials. *Mater. Today Sustainability* **2020**, *7-8*, No. 100028.

(28) Röhrl, M.; Ködel, J. F.; Timmins, R. L.; Callsen, C.; Aksit, M.; Fink, M. F.; Seibt, S.; Weidinger, A.; Battagliarin, G.; Ruckdäschel, H.; Schobert, R.; Breu, J.; Biersack, B. New Functional Polymer Materials via Click Chemistry-Based Modification of Cellulose Acetate. *ACS Omega* **2022**, *8*, 9889−9895.

(29) Lucia, L. A.; Ayoub, A.*Polysaccharide-Based Fibers and Composites: Chemical and Engineering Fundamentals and Industrial Applications*; Springer, 2017; pp 1−117.

(30) Arumughan, V.; Nypelö, T.; Hasani, M.; Larsson, A. Fundamental Aspects of the Non-Covalent Modification of Cellulose via Polymer Adsorption. *Adv. Colloid Interface Sci.* **2021**, *298*, 102529−102529.

(31) Modification of Solid Polysaccharide with Transesterification Agent. 2011.

(32) Dutta, S.; Yu, I. K. M.; Tsang, D. C. W.; Fan, J.; Clark, J. H.; Jiang, Z.; Su, Z.; Hu, C.; Poon, C. S. Efficient Depolymerization of Cellulosic Paper Towel Waste Using Organic Carbonate Solvents. *ACS Sustainability Chem. Eng.* **2020**, *8*, 13100−13110.

(33) Reddy, B. R.; Patil, R.; Patil, S. Chemical Modification of Biopolymers to Design Cement Slurries with Temperature-Activated Viscosification-a Laboratory Study. *SPE Drill. Completion* **2012**, *27*, 94−102.

(34) Nguyen, M. N.; Kragl, U.; Barke, I.; Lange, R.; Lund, H.; Frank, M.; Springer, A.; Aladin, V.; Corzilius, B.; Hollmann, D. Coagulation Using Organic Carbonates Opens up a Sustainable Route towards Regenerated Cellulose Films. *Commun. Chem.* **2020**, *3*, No. 116.

(35) Niu, T.; Wang, X.; Wu, C.; Sun, D.; Zhang, X.; Chen, Z.; Fang, L. Chemical Modification of Cotton Fabrics by a Bifunctional Cationic Polymer for Salt-Free Reactive Dyeing. *ACS Omega* **2020**, *5*, 15409−15416.

https://doi.org/10.1021/acsomega.3c02974
ACS Omega 2023, 8, 25453−25466

(36) Pornpitchanarong, C.; Rojanarata, T.; Opanasopit, P.; Ngawhirunpat, T.; Bradley, M.; Patrojanasophon, P. Maleimide-Functionalized Carboxymethyl Cellulose: A Novel Mucoadhesive Polymer for Transmucosal Drug Delivery. *Carbohydr. Polym.* **2022**, *288*, No. 119368.
(37) (PDF) Mark-Houwink parameters for aqueous-soluble polymers and biopolymers at various temperatures. (accessed February 15, 2023).
(38) Kasaai, M. R. Calculation of Mark−Houwink−Sakurada (MHS) Equation Viscometric Constants for Chitosan in Any Solvent−Temperature System Using Experimental Reported Viscometric Constants Data. *Carbohydr. Polym.* **2007**, *68*, 477−488.
(39) Ouaer, H.; Gareche, M. The Rheological Behaviour of a Water-Soluble Polymer (HEC) Used in Drilling Fluids. *J. Braz. Soc. Mech. Sci. Eng.* **2018**, *40*, No. 380.
(40) Harding, S. E. The Intrinsic Viscosity of Biological Macromolecules. Progress in Measurement, Interpretation and Application to Structure in Dilute Solution. *Prog. Biophys. Mol. Biol.* **1997**, *68*, 207−262.
(41) Yusuf, S. M.; Junin, R.; Sidek, M. A. M.; Agi, A.; Fuad, M. F. I. A.; Rosli, N. R.; Rahman, N. A.; Yahya, E.; Wong, N. A. M S.; Mustaza, M. H. Screening the Synergy of Sodium Dodecylbenzenesulfonate and Carboxymethyl Cellulose for Surfactant-Polymer Flooding. *Pet. Res.* **2022**, *7*, 308−317.
(42) Hebeish, A.; El-Rafie, M. H.; EL-Sheikh, M. A.; El-Naggar, M. E. Ultra-Fine Characteristics of Starch Nanoparticles Prepared Using Native Starch With and Without Surfactant. *J. Inorg. Organomet. Polym. Mater.* **2014**, *24*, 515−524.
(43) Parid, D. M.; Aliaa, N.; Rahman, A.; Baharuddin, A. S.; Mohammed, A. P.; Johari, A. M.; Zubaidah, S.; Razak, A. Synthesis and characterization of carboxymethyl cellulose from oil palm empty fruit bunch stalk fibres. *BioResources* **2018**, *13*, 535−554.
(44) Indran, S.; Raj, R. E.; Sreenivasan, V. S. Characterization of New Natural Cellulosic Fiber from Cissus Quadrangularis Root. *Carbohydr. Polym.* **2014**, *110*, 423−429.
(45) Figueiredo, L. R. F.; Nepomuceno, N. C.; Melo, J. D. D.; Medeiros, E. S. Glycerol-Based Polymer Adhesives Reinforced with Cellulose Nanocrystals. *Int. J. Adhes. Adhes.* **2021**, *110*, No. 102935.
(46) Jamari, S. S.; Howse, J. R. The Effect of the Hydrothermal Carbonization Process on Palm Oil Empty Fruit Bunch. *Biomass Bioenergy* **2012**, *47*, 82−90.
(47) El-hoshoudy, A. N.; Desouky, S. M.; Attia, A. M. Synthesis of Starch Functionalized Sulfonic Acid Co-Imidazolium/Silica Composite for Improving Oil Recovery through Chemical Flooding Technologies. *Int. J. Biol. Macromol.* **2018**, *118*, 1614−1626.
(48) dos Santos, R. M.; Neto, W. P. F.; Silvério, H. A.; Martins, D. F.; Dantas, N. O.; Pasquini, D. Cellulose Nanocrystals from Pineapple Leaf, a New Approach for the Reuse of This Agro-Waste. *Ind. Crops Prod.* **2013**, *50*, 707−714.
(49) Zhang, J.; Wu, D. Characteristics of the Aqueous Solution of Carboxymethyl Starch Ether. *J. Appl. Polym. Sci.* **1992**, *46*, 369−374.
(50) Microcrystalline Cellulose (MCC) from oil palm empty fruit bunch (EFB) fiber via simultaneous ultrasonic and alkali treatment | Request PDF. (accessed February 06, 2023).
(51) Fang, J. M.; Fowler, P. A.; Tomkinson, J.; Hill, C. A. S. The Preparation and Characterisation of a Series of Chemically Modified Potato Starches. *Carbohydr. Polym.* **2002**, *47*, 245−252.
(52) Yeng, L. C.; Wahit, M. U.; Othman, N. Thermal and Flexural Properties of Regenerated Cellulose (RC)/ Poly (3Hydroxybutyrate) (PHB)Biocomposites. *J. Teknol.* **2015**, *75*, 107−112.
(53) Hong, S. M.; Hwang, S. H. Synthesis and Characterization of Multifunctional Secondary Thiol Hardeners Using 3-Mercaptobutanoic Acid and Their Thiol-Epoxy Curing Behavior. *ACS Omega* **2022**, *7*, 21987−21993.
(54) El-hoshoudy, A. N. Experimental and Theoretical Investigation for Synthetic Polymers, Biopolymers and Polymeric Nanocomposites Application in Enhanced Oil Recovery Operations. *Arabian J. Sci. Eng.* **2022**, *47*, 10887−10915.
(55) Lashari, N.; Ganat, T.; Elraies, K. A.; Ayoub, M. A.; Kalam, S.; Chandio, T. A.; Qureshi, S.; Sharma, T. Impact of Nanoparticles Stability on Rheology, Interfacial Tension, and Wettability in Chemical Enhanced Oil Recovery: A Critical Parametric Review. *J. Pet. Sci. Eng.* **2022**, *212*, No. 110199.
(56) Muther, T.; Qureshi, H. A.; Syed, F. I.; Aziz, H.; Siyal, A.; Dahaghi, A. K.; Negahban, S. Unconventional Hydrocarbon Resources: Geological Statistics, Petrophysical Characterization, and Field Development Strategies. *J. Pet. Explor. Prod. Technol* **2022**, *12*, 1463−1488.
(57) Jang, H. Y.; Zhang, K.; Chon, B. H.; Choi, H. J. Enhanced Oil Recovery Performance and Viscosity Characteristics of Polysaccharide Xanthan Gum Solution. *J. Ind. Eng. Chem.* **2015**, *21*, 741−745.
(58) El-hoshoudy, A. N. Synthesis of Acryloylated Starch-g-Poly Acrylates Crosslinked Polymer Functionalized by Emulsified Vinyltrimethylsilane Derivative as a Novel EOR Agent for Severe Polymer Flooding Strategy. *Int. J. Biol. Macromol.* **2019**, *123*, 124−132.
(59) Uschanov, P.; Johansson, L. S.; Maunu, S. L.; Laine, J. Heterogeneous Modification of Various Celluloses with Fatty Acids. *Cellulose* **2011**, *18*, 393−404.
(60) Tundo, P.; Selva, M. The Chemistry of Dimethyl Carbonate. *Acc. Chem. Res.* **2002**, *35*, 706−716.
(61) Reddy, B. In *Viscosification-on-Demand: Chemical Modification of Biopolymers to Control Their Activation by Triggers in Aqueous Solutions*, SPE International Symposium on Oilfield Chemistry; OnePetro, 2011.

https://doi.org/10.1021/acsomega.3c02974
ACS Omega 2023, 8, 25453−25466